

Can Ballistic Electrons Probe the Electronic Spectra of Individual Buried Molecules?

George Kirczenow

Department of Physics, Simon Fraser University, Burnaby, British Columbia, Canada V5A 1S6

(Dated: March 23, 2002)

A theoretical study is presented of the ballistic electron emission spectra (BEES) of individual insulating and conducting organic molecules chemisorbed on a silicon substrate and buried under a thin gold film. It is predicted that ballistic electrons injected into the gold film from a scanning tunneling microscope tip should be transmitted so weakly to the silicon substrate by alkane molecules of moderate length (decane, hexane) and their thiolates that individual buried molecules of this type will be difficult to detect in BEES experiments. However, resonant transmission by molecules containing unsaturated C-C bonds or aromatic rings is predicted to be strong enough for BEES spectra of individual buried molecules of these types to be measured. Calculated BEES spectra of molecules of both types are presented and the effects of some simple interstitial and substitutional gold defects that may occur in molecular films are also briefly discussed.

PACS numbers: 81.07.Nb, 73.63.-b, 81.07.Pr, 73.23.Ad

I. INTRODUCTION

During the last decade there has been growing interest in molecular electronics, stimulated largely by the experimental realization of molecular wires^{1,2,3}, systems in which a single organic molecule or a few molecules carry an electric current between a pair of metal contacts. Hybrid molecule/silicon nanoelectronic devices are another intriguing possibility and research that may lead to their creation is also being pursued.^{4,5,6,7,8,9,10,11,12} For many potential nanoelectronic applications it will be necessary to sandwich a molecular layer between metal and/or semiconductor layers that act as contacts and also protect the molecular layer from the environment. However, this makes the molecules inaccessible to direct nanoscopic experimental probes such as the scanning tunneling microscope (STM). Thus the structures and electronic properties of such buried molecular layers are, to a large degree, still the subject of conjecture.

Ballistic electron emission microscopy (BEEM) is a technique that can probe the nanoscale spatial structure and electronic spectra of buried interfaces.^{13,14} In BEEM experiments a bias voltage is applied between an STM tip and a thin metal overlayer covering a buried substrate, usually a semiconductor, which is kept at almost the same electrochemical potential as the metal overlayer.¹⁵ Electrons are injected from the STM tip into the metal layer and travel ballistically through the metal. Some of them are transmitted through the metal/semiconductor interface into the semiconductor substrate. The electric current transmitted through the interface is measured as a function of both the lateral position of the STM tip and the bias voltage applied between the tip and metal overlayer. This allows the imaging of defect structures at the interface and spatially-resolved spectroscopy of their electronic structure, with nanometer resolution. Recently BEEM experiments have been initiated on systems in which self-assembled molecular monolayers are present between the metal overlayer and semiconductor, specifically, alkane dithiolates between GaAs and gold.¹⁶

Since in such BEEM experiments a significant bias is not applied across the molecular layer, BEEM spectroscopy (BEES) of buried molecules (unlike the usual spectroscopies based on measurements of current-voltage characteristics of molecular diodes^{1,2,3}) is not subject to complications due to bias-induced charging effects and electric fields in or near the molecular layer. Thus in addition to being a unique probe of buried structures with nanometer spatial resolution, BEEM can provide important spectroscopic information relevant to molecular electronics that is complementary to that obtained from measurements of diode current-voltage characteristics. However, because of the absence to date of any appropriate theory, it has been difficult to interpret the results of BEEM experiments for metal/molecule/semiconductor systems unambiguously: For example, in the recent experimental study¹⁶ a BEEM signal could only be detected in a few small, isolated patches of the sample and it has been unclear whether this should be interpreted as evidence that most of the sample was occupied by an insulating alkane-dithiolate self-assembled monolayer (SAM) that did not transmit a detectable BEEM signal and that the observed signal was coming from occasional patches of defects in this SAM, or that to the contrary the detected BEEM signal was being transmitted through small patches of alkane-dithiolate SAM surrounded by much larger regions of a more strongly insulating material (such as alkane-dithiol multilayers) between the semiconductor and the gold overlayer.

In this article a theoretical study is presented of ballistic electron emission microscopy/spectroscopy of single organic molecules between a thin gold overlayer and a silicon substrate. It is predicted that alkane molecules of moderate size (hexane and decane are studied) attached to the Si substrate by a C-Si bond (and whether thiol-bonded or not chemically bonded to the gold overlayer) should transmit the ballistic electrons so weakly that such single molecules are expected to be below the threshold of detection for conventional BEEM equipment. However, related single molecules containing unsaturated C-

C bonds or aromatic rings are predicted to exhibit sufficiently strong transmission resonances that their observation in BEEM experiments should be feasible. Thus it is predicted that *single* molecules with unsaturated C-C bonds or aromatic rings embedded in an alkane or alkane thiolate SAM between a silicon substrate and gold overlayer should be detectable in BEEM experiments with present day equipment. The calculated BEEM spectra of the molecules are also presented and the effects of some simple interstitial and substitutional gold defects that may occur in molecular films are also briefly discussed.

This paper is organized as follows: The theoretical model of the structures and electronic structures of the systems studied and the approach used to calculate the BEEM currents in these systems are described in Section II. The results obtained are presented together with their interpretation and implications for experiment in Section III. The main conclusions are summarized in Section IV.

II. MODEL AND THEORETICAL APPROACH

A. Extended Molecule

As in other transport calculations in molecular electronics,^{3,10,12,17,18,19,20,22,23} the theoretical model studied is based on an *extended molecule* that includes the molecule itself as well as clusters of nearby atoms belonging to the electrodes that transmit electrons to and from the molecule. In this way the chemical bonding between the molecule and the electrodes is taken into account as well as the electronic structures of the molecule and the electrodes. In the present systems there are three electrodes: the STM tip, the metal layer between the tip and the molecule, and the silicon substrate. An atomic cluster from each of these is included in the extended molecule, as is shown for an ethylmethylbenzene molecule in Fig.1: A cluster of 10 Au atoms represents the (111)-oriented monoatomic Au tip. The Au film between the tip and molecule is represented by a 591 Au atom cluster that is approximately cylindrical and presents (111)-oriented facets to the STM tip and the molecule. A hemispherical 390 Si atom cluster with the dangling Si bonds passivated by H atoms and its flat (111) surface facing the molecule represents the Si substrate. The molecules studied here bond to the Si substrate through a single covalent C-Si bond. For those molecules that are thiol-bonded to the gold film, the sulfur atom is positioned $\sim 2.2\text{\AA}$ below a hollow site between three gold surface atoms. Density functional theory was used to estimate the atomic geometries of the molecules and of their bonding to the semiconductor substrate and metal overlayer.²⁶ However in cases where the end of the molecule adjacent to the gold layer terminates in a CH_3 group (which does not bond to the gold), the distance between the gold surface plane and the closest H atom of the molecule is somewhat arbitrary, and was assumed to be 3\AA .

B. Electronic Structure

Most theoretical work on electronic transport in molecular wires with metal contacts has been based on semi-empirical tight-binding models or Kohn-Sham density functional calculations of the electronic structure.^{3,17,18,19,20,22,23} It was found in the present study that, in order to realistically model ballistic transmission of electrons through the gold film between the STM tip and molecule in BEEM experiments, several hundred Au atoms need to be included in the cluster that represents the gold film in extended molecule. This makes the density functional approach impractical for the transport problem. Furthermore previous theoretical work modeling the current-voltage characteristics of molecules on silicon found Kohn-Sham density functional calculations to be unsuitable for treating the electronic structure of the silicon substrate,¹⁰ and to yield results that disagree qualitatively with experimental STM data.¹² However, transport calculations based on semi-empirical tight-binding models can be performed for systems with large numbers of atoms and have successfully explained experimental current-voltage characteristics of molecules connecting gold electrodes^{3,18,20} and of molecular wires on silicon substrates.¹² Thus a hybrid tight-binding model of the electronic structure that combines parameters derived from semi-empirical considerations of quantum chemistry and from *ab initio* band structure calculations is adopted here. As is explained below, a number of parameters that enter the model are not known accurately, and in order to proceed further it is necessary to make plausible but not rigorous approximations and assumptions regarding their values. The sensitivity of the present findings to the values of these parameters was explored in the course of this work and it was found that the *qualitative* conclusions reported here are robust to reasonable variations in parameter values. The reader is referred to previous papers^{12,23,24} for extended discussions of the reliability of such techniques.

The semi-empirical extended Hückel model of quantum chemistry^{27,28} is used to describe the electronic structure of the molecule and coupling between the molecule and silicon substrate. However in order to model the electronic structure of the silicon substrate satisfactorily, the extended Hückel model requires modification and this is done here as in Ref.12: Extended Hückel theory describes molecular systems in terms of a small set of Slater-type atomic orbitals $\{|\phi_i\rangle\}$, their overlaps $S_{ij} = \langle\phi_i|\phi_j\rangle$ and a Hamiltonian matrix $H_{ij} = \langle\phi_i|H|\phi_j\rangle$. The diagonal Hamiltonian elements $H_{ii} = \epsilon_i$ are the atomic orbital ionization energies. Non-diagonal elements are approximated by

$$H_{ij} = KS_{ij}(\epsilon_i + \epsilon_j)/2 \quad (1)$$

where K is a phenomenological parameter usually chosen to be 1.75 for consistency with experimental molecular electronic structure data. However, in the present work, as is discussed in detail in Ref.12, for Si atoms

the single parameter K is replaced by a set of parameters K_{ij} whose values are chosen so that the modified extended Hückel model obtained in this way yields an accurate description of the band structure of crystalline silicon. The electronic structures of the gold film and STM tip are also described by a tight-binding model with a non-orthogonal basis but in this case the tight-binding parameters H_{ij} and S_{ij} from Ref. 29 that are based on fits to *ab initio* calculations of the electronic structure of gold are used. The atomic orbital energies H_{ii} of Ref. 29 for gold are defined up to an arbitrary additive constant which is chosen in the present work so as to yield reasonable values of the energy offsets $\Delta_{M,Au}$ between the HOMO levels of the molecules M studied and the Fermi level of the gold film. The values of the offsets $\Delta_{M,Au}$ are not known accurately at present either theoretically or experimentally, their determination being an important open problem of molecular electronics. For the present purpose they are estimated as the differences between the work function of Au and the HOMO energies of the respective isolated molecules obtained from density functional theory, an approximation that has been used successfully to align the Fermi energy of gold with the HOMO of benzenedithiolate,³⁰ and has also been applied to a variety of other metal-molecule junctions.²³ The effects of the potential difference between the STM tip and the gold film on the electronic structure of the system are included in the present model by offsetting the atomic orbital energies H_{ii} for gold STM tip upwards in energy from those of the gold film by an amount $|eV|$ where V is bias voltage between the tip and Au film. The value of the energy offset $\Delta_{Si,Au}$ of the silicon conduction band edge (at the surface of the silicon substrate) above the Fermi level of the gold film is another important parameter that is not known accurately for gold/molecule/silicon heterojunctions. Here it is assumed, for simplicity, that $\Delta_{Si,Au} = 0.84\text{eV}$, a typical experimental value of the Schottky barrier measured in BEEM experiments on Au/Si(111) interfaces;³¹ the Si orbital energies $H_{ii} = \epsilon_i$ are adjusted (all equally) so as to place the LUMO level of the Si cluster of the extended molecule 0.84eV above the Fermi level of the gold film. Finally, the Hamiltonian matrix elements between the STM tip and gold film and between the gold film and molecule are estimated from Eq.(1) with $K = 1.75$. Because of the non-orthogonality of the basis states employed in the present model, the above adjustments of the diagonal matrix elements H_{ii} of the tight binding Hamiltonian require^{12,21} corresponding adjustments ΔH_{ij} of the non-diagonal elements H_{ij} , which were taken to be

$$\Delta H_{ij} = S_{ij}(E_i + E_j)/2 \quad (2)$$

where E_k is the shift of the diagonal element H_{kk} .

C. Transport

In a BEEM experiment the electron flux that passes from the STM tip to the gold film subsequently separates: A small part of it (that constitutes the BEEM current I_{BEEM}) continues through the molecule to the Si substrate and on to the electron drain electrode, while most of it (referred to henceforth as the film current I_{FILM}) proceeds laterally through the gold film directly to the drain electrode. The total current I_{tip} passing through the STM tip is thus given by $I_{\text{tip}} = I_{\text{BEEM}} + I_{\text{FILM}}$.

The present calculations of I_{BEEM} and I_{FILM} are based on Landauer-Büttiker theory.³² For BEEM experiments the gold film, the Si substrate and the electron drain can all be considered to be at the same electrochemical potential.¹⁵ Also, in practice, electron transmission from the source to drain via the gold film, molecule and silicon substrate, and directly via the gold film are mutually incoherent processes. Therefore it follows from Landauer-Büttiker theory that the currents I_{BEEM} and I_{FILM} at a given value of the applied source-drain bias voltage V are related to the multichannel electron transmission probabilities $T_x(E, V)$ at energy E from the source electrode to the drain via x where x can be the BEEM path through the gold film, molecule and Si substrate ($x = \text{BEEM}$), or the direct path through the gold film to the drain ($x = \text{FILM}$), according to

$$I_x(V) = -\frac{2e}{h} \int_{-\infty}^{\infty} dE T_x(E, V) (f(E, \mu_s) - f(E, \mu_d)) \quad (3)$$

where $f(E, \mu_i) = 1/(\exp[(E - \mu_i)/kT] + 1)$ and μ_i is the electrochemical potential of the source ($i = s$) or drain ($i = d$) electrode.³³

The source and drain electrodes are modelled here as arrays of ideal single-channel leads: One such drain lead is coupled to the $1s$ orbital of each of the hydrogen atoms that passivate the dangling bonds terminating the Si cluster of the extended molecule, and one is coupled to each p valence orbital of the surface atoms of the Si cluster (except for those of the H and Si atoms in the vicinity of the Si atom to which the molecule bonds), a total of 675 ideal leads. An ideal drain lead is also coupled to each s , p and d valence orbital of the surface atoms of the Au cluster representing the Au film, except for those Au atoms in the immediate vicinity of the molecule and STM tip, totalling 2709 leads. Similarly an ideal source lead is coupled to each valence s , p and d orbital of the surface atoms of the cluster representing the STM tip, except for the terminal atom of the tip, a total of 81 leads. Each ideal lead k was modelled as a semi-infinite tight-binding chain with a single orbital per site, a site energy α_k and nearest neighbor hopping matrix element β . α_k was chosen to be equal to the energy (including the shift, if any, due to the applied bias) of the hydrogen, silicon or gold orbital to which lead k was coupled. The hopping matrix elements β were all taken to have a magnitude of 6 eV, sufficiently large that the eigenmodes of all of the ideal

leads in the energy window between μ_s and μ_d in eq. (3) be composed of counter-propagating (left and right moving) waves. The coupling matrix elements W_k between the ideal leads and their respective hydrogen, silicon and gold orbitals were also set to β .

As well as mimicking macroscopic electrodes by transmitting an ample electron flux to and from the system, the above large numbers of ideal source and drain leads have a similar effect to phase-randomizing Büttiker probes³⁴ in minimizing the influence of dimensional resonances due to the finite sizes of the gold and silicon clusters employed in the model; it was verified that the ideal leads described above meet these requirements by comparing the results obtained in test calculations with differing numbers of ideal leads, differing values of the lead parameters, and differing numbers of atoms in the Au and Si clusters of the extended molecules. Calculations of the currents I_{BEEM} and I_{FILM} for cylindrical Au atom clusters with the same height (1.4nm) as that of the 591 Au atom cluster in Fig.1 but with differing diameters confirmed that the diameter of this cluster (approximately 2.5nm) was sufficient for these currents to have converged with increasing cluster diameter, i.e., that electron transport through this finite cluster adequately represents ballistic propagation of electrons through a thin but laterally extended gold film.

To calculate $T_x(E, V)$ and hence evaluate eq.(3), the transformation to the alternate Hilbert space described in Refs. 35 and³⁶ was made, mapping the non-orthogonal basis of atomic orbitals to an orthogonal basis. The Lippmann-Schwinger equation

$$|\Psi_k\rangle = |\Phi_{o,k}\rangle + G_o(E)W|\Psi_k\rangle \quad (4)$$

describing electron scattering between the source and drain leads was solved numerically for $|\Psi_k\rangle$ in the alternate Hilbert space.^{35,36} In eq.(4) $G_o(E)$ is the Green's function for the decoupled system (i.e., with the coupling between the ideal leads and the extended molecule switched off), $|\Phi_{o,k}\rangle$ is the eigenstate of the decoupled ideal source lead k with energy E and $|\Psi_k\rangle$ is the corresponding scattering eigenstate of the complete system with the coupling W between the ideal leads and the extended molecule switched on. The scattering amplitudes t_{jk} from the ideal source lead k to drain lead j at energy E were extracted from the scattering eigenstates $|\Psi_k\rangle$ and the transmission probabilities that enter eq. (3) were then calculated from

$$T_x(E, V) = \sum_k \sum_j \left| \frac{v_j}{v_k} \right| |t_{jk}|^2 \quad (5)$$

where v_k and v_j are the electron group velocities in ideal leads k and j respectively at energy E . The sum over j in Eq. (5) is over those drain leads connected to electrode x , i.e., the gold metal film or the Si substrate as discussed above, while that over k is over the leads connected to the STM tip.

III. RESULTS

For the terminal atom of the gold STM tip over an atom at the center of the top surface of the Au cluster that represents the gold film in Fig.1, and separated from that surface atom by a nearest neighbor distance of gold (2.88Å), the STM tip and gold film are connected by an atomic quantum point contact. For this geometry the present calculations of the electron transmission probability $T_{\text{FILM}}(E, 0)$ between the tip and gold film at zero applied bias yield values close to 1 (per spin) for energies E around the Fermi level of gold, consistent with previous experimental^{37,38} and theoretical^{38,39} studies of gold atomic point contacts. However, in BEEM experiments the STM tip is normally further from the gold film, at distances in the STM tunneling regime. Unless stated otherwise, the results of the BEEM calculations to be presented here will be for such a larger separation (4.33Å) between the tip atom and the gold film for which the calculated the electron transmission probability $T_{\text{FILM}}(E_F, 0)$ between the tip and gold film at the gold Fermi energy and zero applied bias is approximately 10^{-2} . The calculated electron transmission probabilities $T_{\text{BEEM}}(E, V)$ from the electron source to the drain via the STM tip, gold film, molecule and silicon substrate are shown in Fig. 2 for two representative molecules that are shown in the insets. The solid (dotted) curves are for zero (2V) bias V between the STM tip and gold film. The Fermi level of the gold film is at $E=0$ in all cases, and the silicon conduction band edge at the silicon surface E_C is indicated by the vertical dashed line. The lower plot is for decanethiolate ($\text{C}_{10}\text{H}_{20}\text{S}$) thiol bonded to the gold film below a hollow site between 3 gold atoms and attached to the silicon substrate by a single carbon-silicon bond. This molecule is insulating, having a large HOMO-LUMO gap, and thus its transmission in a BEEM experiment is predicted to be very small resulting in $T_{\text{BEEM}}(E, V) \leq 10^{-11}$ in the range shown. The upper plot is for another chain molecule ($\text{C}_{10}\text{H}_{18}\text{S}$) also with 10 carbon atoms and bonded similarly to the gold film and Si substrate, but in this case the 5th and 6th carbon atoms each have one H atom attached instead of two so that there is a double bond connecting these two C atoms; see upper inset. This double C-C bond gives rise to a molecular state near $E = 1.65\text{eV}$ where the transmission $T_{\text{BEEM}}(E, V)$ is greatly enhanced (at its peak by almost seven orders of magnitude relative to that for the decanethiolate) although it is still *very* weak ($< 10^{-5}$) in absolute terms, as expected for a transmitting state associated with a double bond surrounded by large potential barriers. However, there is no other resonantly transmitting state in this system in the energy range above and reasonably close to the Fermi level of the gold film, the range relevant to BEEM experiments. Therefore despite its weakness this resonance is the dominant BEEM transport mechanism for this system as will be seen below. Notice that the application of a 2V bias does not change the transmission probabilities $T_{\text{BEEM}}(E, V)$ by much on

the scale of Fig. 2 (less than a factor of 2) because the main transport bottleneck here is the molecule and the application of a bias between the tip and gold film does not affect the molecule significantly.

In BEEM experiments the distance between the tip and gold film is not known accurately, as is the case for most STM experiments where only *changes* in the tip-surface separation are measured. However, the transmission probabilities T_{BEEM} and T_{FILM} and currents I_{BEEM} and I_{FILM} depend strongly on the tip-surface separation. This makes a direct comparison between calculated and experimental values of these quantities problematic. However, it is intuitively plausible that I_{BEEM} and I_{FILM} should scale in the same way with the tip-surface separation in the tunneling regime and thus $I_{\text{BEEM}}/I_{\text{FILM}}$ should be nearly independent of the tip-surface separation. This has been confirmed by calculations carried out in the present study. Thus the ratio $I_{\text{BEEM}}/I_{\text{FILM}}$ lends itself better than I_{BEEM} or I_{FILM} to comparison between theory and experiment and it will therefore be the focus of attention in what follows. Another advantage of studying this quantity theoretically is that spectroscopic BEEM (i.e. BEES) measurements of I_{BEEM} vs. the bias voltage applied between the STM tip and metal film are normally taken not at constant tip-surface separation but at constant tip current I_{tip} , which, for the systems studied here, differs negligibly from the film current I_{FILM} . Therefore because $I_{\text{BEEM}}/I_{\text{FILM}}$ is approximately independent of the tip-surface separation, plots of $I_{\text{BEEM}}/I_{\text{FILM}}$ vs. bias voltage should differ from experimental plots of I_{BEEM} vs. bias by only a scale factor that is independent of the bias, making qualitative comparisons between calculations and BEES current-voltage characteristics appropriate. A typical experimental BEEM setup can readily detect BEEM currents with current ratios $I_{\text{BEEM}}/I_{\text{tip}}$ greater than roughly 10^{-5} ; this number will be referred to below as the “nominal BEEM sensitivity threshold” (NBT).

In the present calculations the silicon cluster that represents the silicon substrate in the extended molecule is of necessity small even though it includes hundreds of atoms; the silicon hemisphere shown in Fig.1 has a radius slightly less than 1.5nm. Because of its small size it transmits electrons appreciably by quantum tunneling even at energies below the conduction band edge E_C in Fig.2 where there are no eigenstates of the extended molecule with a strong silicon content. Because of this the calculated transmission $T_{\text{BEEM}}(E, V)$ shown in in Fig.2, although it is extremely weak below E_C , does not decline all the way to zero for $E < E_C$. Thus while the present model should describe the BEEM electron transmission reasonably well at energies higher than E_C , it does not describe the details of the *onset* of BEEM current at the threshold voltage $V = E_C$ accurately for macroscopic silicon substrates. However, as will be seen below, for the molecules studied here, the current ratios $I_{\text{BEEM}}/I_{\text{tip}}$ in the near-threshold regime are very far below nominal BEEM sensitivity threshold, and detailed study of this

regime is therefore left for future work. Here, for simplicity, in calculating I_{BEEM} from Eq. (3), $T_{\text{BEEM}}(E, V)$ will be set to zero for $E < E_C$.

The calculated current ratios $I_{\text{BEEM}}/I_{\text{tip}}$ for some representative saturated chain molecules are shown in Fig. 3. $\text{C}_{10}\text{H}_{21}$ is decane bonded to the silicon substrate through a single C-Si bond and not bonded chemically to the gold film. Even at an STM tip bias of 4V the calculated $I_{\text{BEEM}}/I_{\text{tip}}$ for this molecule is 6 orders of magnitude below the nominal BEEM sensitivity threshold. For $\text{C}_{10}\text{H}_{20}\text{S}$ (decanethiolate depicted in the lower inset of Fig. 2) the thiol bond to the Au film results in predicted BEEM currents two orders of magnitude larger than for $\text{C}_{10}\text{H}_{21}$. However, the calculated current ratios $I_{\text{BEEM}}/I_{\text{tip}}$ for both $\text{C}_{10}\text{H}_{21}$ and $\text{C}_{10}\text{H}_{20}\text{S}$ are still so low as to be well below the NBT not only for single molecules but even for self-assembled molecular monolayers where hundreds of molecules may be contributing together to the BEEM current. For $\text{C}_6\text{H}_{12}\text{S}$ (hexanethiolate which is similar to decanethiolate but with fewer carbon atoms and so presents a thinner tunnel barrier than decanethiolate) the calculated current ratios $I_{\text{BEEM}}/I_{\text{tip}}$ are two orders of magnitude higher than for decanethiolate but still well below the NBT. Thus detecting a BEEM signal from single alkane or alkanethiolate molecules on silicon or even from self-assembled monolayers of these molecules is expected to be challenging experimentally except for quite short molecules of these types. This is quite reasonable given the well known insulating nature of alkanes and alkanethiols.

While the solid curves in Fig. 3 are for a separation of 4.33Å between the STM tip atom and the gold film, the (black) dotted curve for $\text{C}_6\text{H}_{12}\text{S}$ is for a 5.05Å separation at which the calculated transmission T_{FILM} between the STM tip and gold film is lower by a factor of approximately 35. Notice that the calculated values of $I_{\text{BEEM}}/I_{\text{tip}}$ are almost the same for the two separations, illustrating the insensitivity of the ratio $I_{\text{BEEM}}/I_{\text{tip}}$ to the separation between the STM tip and gold film in the tunneling regime, as has been discussed above.

The calculated current ratios $I_{\text{BEEM}}/I_{\text{tip}}$ for some representative unsaturated molecules are shown in Fig. 4. Transmission resonances due to molecular states associated with the unsaturated C-C bonds in these molecules give rise to dramatic increases in the BEEM current at bias voltages (indicated by arrows) at which the Fermi level of the STM tip crosses the resonant molecular energy levels. As a result, even for $\text{C}_{10}\text{H}_{18}\text{S}$ (depicted in the upper inset of Fig. 2) the largest value of $I_{\text{BEEM}}/I_{\text{tip}}$ is predicted to be within an order of magnitude of the NBT. For $\text{C}_6\text{H}_{10}\text{S}$ (similar to $\text{C}_{10}\text{H}_{18}\text{S}$ but with a shorter C chain and only one H atom bonded to C atoms 3 and 4) and for C_9H_{11} (ethylmethylbenzene depicted in Fig. 1) $I_{\text{BEEM}}/I_{\text{tip}}$ is predicted to exceed the NBT for bias voltages above the threshold for resonant transport.⁴⁰ Thus experimental observation of single buried molecules such as these in BEEM experiments should be feasible with conventional BEEM equipment. Because the predicted

current ratios $I_{\text{BEEM}}/I_{\text{tip}}$ for saturated molecules (Fig. 3) are much smaller than those for unsaturated molecules of similar length (Fig. 4) it should be possible to study individual buried unsaturated molecules by BEEM and BEES by including a few unsaturated molecules in a self-assembled monolayer of saturated molecules of similar size on silicon under a thin gold film, the saturated molecules behaving as an insulating background surrounding the unsaturated conducting molecules. I.e., BEEM and BEES experiments extending to *buried* single molecules the classic STM studies^{1,41} of the properties of single unsaturated molecules embedded in self-assembled monolayers of saturated molecules on gold substrates should be feasible. However, in interpreting such experiments it is important to note that the calculated current ratios $I_{\text{BEEM}}/I_{\text{tip}}$ shown in Fig. 4 for unsaturated molecules rise with increasing bias from values far below the NBT. Because of this, experimentally observed values of the threshold voltage for the onset of the BEEM current are likely to depend on the sensitivity of the BEEM equipment unless equipment capable of detecting extremely weak BEEM currents is used.

As in Fig. 3, the solid curves in Fig. 4 are for a separation of 4.33Å between the STM tip atom and the gold film while the (black) dotted curve for $\text{C}_6\text{H}_{10}\text{S}$ is for a 5.05Å separation at which the calculated transmission T_{FILM} is again lower by a factor of approximately 35. Once again the calculated values of $I_{\text{BEEM}}/I_{\text{tip}}$ are almost the same for the two separations, illustrating the insensitivity of the ratio $I_{\text{BEEM}}/I_{\text{tip}}$ to the separation between the STM tip and gold film in the tunneling regime, this time for a resonantly transmitting molecule.

In the course of the present work, preliminary results have also been obtained for some defects that may occur in molecular SAMS on silicon covered with gold: It was found that small interstitial gold clusters embedded between decanethiolate molecules of the SAM and also single gold atoms substituting for H atoms of decanethiolate molecules should give rise to BEEM transmission resonances and associated features in $I_{\text{BEEM}}/I_{\text{tip}}$ qualitatively similar to shown in Fig. 4. However, these resonant features in T_{BEEM} and I_{BEEM} were found to be much weaker for the defects that were studied (a 6 atom Au cluster roughly equidistant from the Au film and Si substrate and a single gold atom substituting for a H atom on the 5th C atom [from the Si substrate] of decanethiolate) than those of the unsaturated $\text{C}_{10}\text{H}_{18}\text{S}$ molecule.

Finally, it is interesting that the recent experimental studies¹⁶ of gold-covered octanedithiol molecules on GaAs substrates observed BEEM current-voltage characteristics qualitatively similar to the resonant behavior in Fig. 4. However, since the experiments were on saturated molecules and the BEEM signal was observed only in a few very small patches of the sample the origin of the observed behavior is unclear.

IV. CONCLUSIONS

A better understanding of the electronic and structural properties of buried molecular layers and single molecules

is essential for the development of molecular nanoelectronics. In this paper the feasibility of imaging single buried molecules and measuring their electronic spectra has been explored theoretically. It was found that the insulating nature of single alkane and alkanethiolate molecules chemisorbed on silicon substrates and covered with gold should make them difficult to detect by ballistic electron emission microscopy and spectroscopy for all but very short molecules of this kind. However BEEM currents resonantly transmitted through molecules containing double C-C bonds or aromatic rings should be large enough to be accessible to present day BEEM equipment, and predictions of the BEEM current-voltage characteristics for some examples of molecules of each type have been presented. The predicted BEEM current-voltage characteristics for unsaturated molecules exhibit observable features (marked by the arrows in Fig. 4) due to resonantly transmitting electronic states of the extended molecule that lie above the Fermi level of the metal overlayer. The energy differences between these resonant electronic states and the Fermi level of the metal film are given by $|eV|$ where V is the bias voltage between the STM tip and metal film at which such a feature occurs. Thus BEEM current-voltage characteristics can be used to measure the electronic spectra of buried unsaturated molecules in the environment between the metal and semiconductor layers. Since no bias voltage is applied between the metal overlayer and semiconductor substrate that surround the molecule these BEEM spectra differ from those obtained using conventional diode measurements in which the bias voltage is applied *across the molecule* and therefore modifies the electronic structure that is being measured.

At the present time rigorous theoretical techniques for molecular electronics, and especially molecular transport calculations, have yet to be developed. Thus the present study relies on a combination of semi-empirical and *ab-initio* methods as well as intuitively reasonable approximations and assumptions. The results presented should facilitate the design and interpretation of experiments by providing theoretical answers to some rather basic questions regarding BEEM and BEES of molecules that have not been addressed previously. Further theoretical work on this topic as well as experiments testing the present predictions are clearly desirable, and it is hoped that the present exploration will stimulate such efforts.

Acknowledgments

I thank K. Kavanagh and H. Dalglish for discussions. This research was supported by the Canadian Institute for Advanced Research and NSERC.

- ¹ L. A. Bumm, J. J. Arnold, M. T. Cygan, T. D. Dunbar, T. P. Burgin, L. Jones II, D. L. Allara, J. M. Tour, and P. S. Weiss, *Science* **271**, 1705 (1996).
- ² M. A. Reed, C. Zhou, C. J. Muller, T. P. Burgin, and J. M. Tour, *Science* **278**, 252 (1997).
- ³ S. Datta, W. Tian, S. Hong, R. Reifenberger, J. I. Henderson, C. P. Kubiak, *Phys. Rev. Lett.* **79**, 2530 (1997).
- ⁴ G. P. Lopinski, D.D.M. Wayner, R.A. Wolkow, *Nature* **406**, 48 (2000).
- ⁵ J.-H. Cho, D.-H. Oh, and L. Kleinman, *Phys. Rev. B* **65**, 081310(R) (2002).
- ⁶ W. A. Hofer, A. J. Fisher, G. P. Lopinski, R. A. Wolkow, *Chem. Phys. Lett.* **365**, 129 (2002).
- ⁷ N. P. Guisinger, M. E. Greene, R. Basu, A. S. Baluch, and M. C. Hersam, *Nano Letters* **4**, 55 (2004).
- ⁸ X. Tong, G. A. DiLabio, R. A. Wolkow, *Nano Letters* **4**, 979 (2004).
- ⁹ Y. Wang and G. S. Huyang, *Appl. Phys. Lett.* **86**, 023108 (2005).
- ¹⁰ T. Rakshit, G.-C. Liang, A. W. Ghosh, and S. Datta, *Nano Letters* **4**, 1803 (2004).
- ¹¹ P.G. Piva, G.A. DiLabio, J.L. Pitters, J. Zikovsky, M. Rezeq, S. Dogel, W.A. Hofer, R.A. Wolkow, *Nature* **435**, 658 (2005).
- ¹² G. Kirczenow, P. G. Piva and R. A. Wolkow, *Phys. Rev. B* **72**, 245306 (2005).
- ¹³ L.D. Bell, W.J. Kaiser, *Phys. Rev. Lett.* **61**, 2368 (1988).
- ¹⁴ For a recent review of the BEEM literature see V. Narayanamurti, M. Kozhevnikov, *Physics Reports* **349**, 447 (2001).
- ¹⁵ In BEEM experiments there may be a potential difference of a few meV between the semiconductor substrate and the metal overlayer, however, this potential difference is normally much smaller than the potential difference between the STM tip and metal overlayer. Thus its effect on the BEEM current is usually very small and will be neglected in the present theoretical study.
- ¹⁶ W. Li, K. L. Kavanagh, C. M. Matzke, A. A. Talin, F. Léonard, S. Faleev and J. W. P. Hsu, *J. Phys. Chem. B* **109**, 6252 (2005).
- ¹⁷ E. G. Emberly, G. Kirczenow, *Phys. Rev. B* **58**, 10911 (1998); S. N. Yaliraki, M. Kemp, M. A. Ratner, *J. Am. Chem. Soc.* **121**, 3428 (1999); V. Mujica, A. E. Roitberg, M. Ratner, *J. Chem. Phys.* **112**, 6834 (2000); L. E. Hall, J. R. Reimers, N. S. Hush and K. Silverbrook, *J. Chem. Phys.* **112**, 1510 (2000); M. Di Ventra, S. T. Pantelides, and N. D. Lang, *Phys. Rev. Lett.* **84**, 979 (2000); J. Taylor, H. Guo, J. Wang, *Phys. Rev. B* **63**, 121104(R) (2001); P. E. Kornilovitch and A. M. Bratkovsky, *Phys. Rev. B* **64**, 195413 (2001). P. S. Damle, A. W. Ghosh and S. Datta, *Phys. Rev. B* **64**, 201403(R) (2001).
- ¹⁸ E. G. Emberly and G. Kirczenow, *Phys. Rev. Lett.* **87**, 269701 (2001), *Phys. Rev. B* **64**, 235412 (2001).
- ¹⁹ M. Paulsson, S. Stafstrom, *Phys. Rev. B* **64**, 35416 (2001); J. J. Palacios, A. J. Pérez-Jiménez, E. Louis, J. A. Vergés, *Phys. Rev. B* **64**, 115411 (2001); M. H. Hettler, H. Schoeller, W. Wenzel, *Europhys. Lett.* **57**, 571 (2002); J. Taylor, M. Brandbyge, K. Stokbro, *Phys. Rev. Lett.* **89**, 138301 (2002); J. Heurich, J. C. Cuevas, W. Wenzel, G. Schön, *Phys. Rev. Lett.* **88**, 256803 (2002); R. Gutierrez, F. Grossmann, R. Schmidt, *Chemphyschem* **3**, 650 (2002).
- ²⁰ J. G. Kushmerick, D. B. Holt, J. C. Yang, J. Naciri, M. H. Moore, R. Shashidhar, *Phys. Rev. Lett.* **89**, 086802 (2002).
- ²¹ E. G. Emberly, G. Kirczenow, *Chem. Phys.* **281**, 311 (2002).
- ²² M. Zwolak and M. Di Ventra, *Appl. Phys. Lett.* **81**, 925 (2002); E. G. Emberly and G. Kirczenow, *Phys. Rev. Lett.* **91**, 188301 (2003); R. Pati, L. Senapati, P. M. Ajayan, and S. K. Nayak, *Phys. Rev. B* **68**, 100407(R) (2003); Y. Xue and M.A. Ratner, *Phys. Rev. B* **69**, 085403 (2004), *Phys. Rev. B* **70**, 081404 (2004); S.H. Ke, H.U. Baranger, W.T. Yang **70**, 085410 (2004); C.C. Kaun, H. Guo, *Nano Letters* **3**, 1521 (2003); W. I. Babiaczyk and B. R. Bulka, *J. Phys.: Cond. Matt.* **16**, 4001 (2004); A. R. Rocha, V. M. García-Suárez, S. W. Bailey, C. J. Lambert, J. Ferrer, S. Sanvito, *Nature Mat.* **4**, 335 (2005).
- ²³ H. Dalgleish and G. Kirczenow, *Phys. Rev. B* **72**, 184407 (2005), *Nano Letters* **6**, 1274 (2006), *Phys. Rev. B* **73**, 235436, (2006), *Phys. Rev. B* **73**, 245431 (2006).
- ²⁴ D. Kienle, J. I. Cerda, A. W. Ghosh, *J. Appl. Phys.* **100**, 043714 (2006).
- ²⁵ The MacMolPlt graphics package was used. B. M. Bode, and M. S. Gordon, *J. Mol. Graphics Mod.*, **16**, 133 (1998).
- ²⁶ The Gaussian98/03 packages were used.
- ²⁷ S. P. McGlynn, L. G. Vanquickenborne, M. Kinoshita and D. G. Carrol, *Introduction to Applied Quantum Chemistry*, ch. 2-4, Holt, Rinehart, Winston Inc., (1972).
- ²⁸ The YAEHMOP numerical implementation of extended Hückel theory by G. Landrum and W. Glassey was used.
- ²⁹ D. A. Papaconstantopoulos, *Handbook of the Band Structure of Elemental Solids*, Plenum Press, New York, 1986.
- ³⁰ P. A. Derosa and J. M. Seminario, *J. Phys. Chem. B* **105**, 471 (2001).
- ³¹ L.D. Bell, *Phys. Rev. Lett.* **77**, 3893 (1996).
- ³² For a review see S. Datta, *Electronic Transport in Mesoscopic Systems*, Cambridge University Press: Cambridge, 1995.
- ³³ The temperature T in the Fermi functions was set to 0 in the calculations reported here.
- ³⁴ M. Büttiker, *Phys. Rev. B* **33**, 3020 (1986).
- ³⁵ E. G. Emberly and G. Kirczenow, *Phys. Rev. Lett.* **81**, 5205 (1998).
- ³⁶ E. G. Emberly and G. Kirczenow, *J. Phys.: Condens. Matter* **11**, 6911 (1999).
- ³⁷ N. Agraït, J. G. Rodrigo, and S. Vieira, *Phys. Rev. B* **47**, 12345 (1993); J. I. Pascual, J. Méndez, J. Gómez-Herrero, A. M. Baró, N. García, V. T. Binh, *Phys. Rev. Lett.* **71**, 1852 (1993); A. I. Yanson, G. R. Bollinger, J. M. van Ruitenbeek, *Nature (London)* **395**, 783 (1998).
- ³⁸ S. K. Nielsen, M. Brandbyge, K. Hansen, K. Stokbro, J. M. van Ruitenbeek, F. Besenbacher, *Phys. Rev. Lett.* **89**, 066804 (2002); K. Hansen, S. K. Nielsen, M. Brandbyge, E. Lægsgaard, I. Stensgaard, and F. Besenbacher, *Appl. Phys. Lett.* **77**, 708 (2000).
- ³⁹ M. Brandbyge, M. R. Sørensen, and K. W. Jacobsen *Phys. Rev. B* **56**, 14956 (1997); E. Emberly and G. Kirczenow, *Phys. Rev. B* **60**, 6028 (1999).
- ⁴⁰ The two arrows associated with the BEEM current-voltage characteristic of C_9H_{11} in Fig. 4 mark features that are due to transmission resonances associated with the lowest unoccupied molecular orbital (LUMO) and the LUMO+1

orbital of the molecule.

- ⁴¹ Z. J. Donhauser, B. A. Mantooth, K. F. Kelly, L. A. Bumm, J. D. Monnell, J. J. Stapelton, D. W. Prince

Jr., A. M. Rawlett, D. L. Allara, J. M. Tour and P. S. Weiss, *Science* **292**, 2303 (2001).

FIG. 1: (Color on line). The extended molecule studied in the BEEM transport calculations for the case where the molecule is ethylmethylbenzene.²⁵ The STM tip is represented by 10 Au atoms in a (111) geometry and terminates in a single atom. The Au film is represented by a cylindrical cluster of 591 Au atoms in a bulk crystal geometry that presents (111)-oriented facets to the STM tip and the molecule. The substrate is represented by an approximately hemispherical crystallite of 390 Si atoms. The Si dangling bonds are passivated with H atoms and a flat (111) surface faces the molecule. The molecule bonds to the Si substrate through a single C-Si covalent bond. A large number of single channel ideal leads (most of them not shown) representing the source and drain electrodes are attached to the atomic valence orbitals of appropriate surface atoms of the clusters representing the STM tip, Au film, silicon substrate and passivating H atoms.

FIG. 2: (Color on line). Calculated electron transmission probabilities $T_{\text{BEEM}}(E, V)$ from electron source to drain via STM tip, gold film, molecule and silicon substrate vs. electron energy E . Solid (dotted) curves are for at zero (2V) bias V between STM tip and gold film. The gold film Fermi energy is at $E = 0$ and the Si conduction band edge at the Si surface E_C is shown by the dashed vertical line. The lower plots are for the decane thiolate $\text{C}_{10}\text{H}_{20}\text{S}$ molecule in the lower inset. The upper plots are for the $\text{C}_{10}\text{H}_{18}\text{S}$ molecule in the upper inset that exhibits resonant transmission due to the presence of a double C-C bond.

FIG. 3: (Color on line). Calculated BEEM to film current ratios vs. tip bias voltage V for some saturated molecules: Decane ($\text{C}_{10}\text{H}_{22}$), decanethiolate ($\text{C}_{10}\text{H}_{20}\text{S}$) and hexanethiolate ($\text{C}_6\text{H}_{12}\text{S}$). The red horizontal dashed line is the nominal BEEM sensitivity threshold. Solid curves are for a separation of 4.33\AA between the STM tip atom and the gold film. The (black) dotted curve for $\text{C}_6\text{H}_{12}\text{S}$ is for a 5.05\AA separation.

FIG. 4: (Color on line). Calculated BEEM to film current ratios vs. tip bias voltage V for some unsaturated chain molecules $\text{C}_{10}\text{H}_{18}\text{S}$ (shown in the upper inset of Fig. 2) and $\text{C}_6\text{H}_{10}\text{S}$, and for ethylmethyl benzene C_9H_{11} shown in Fig. 1. Arrows indicate values of the bias voltage at which the STM tip Fermi level crosses the energies of molecular resonant states. The red horizontal dashed line is the nominal BEEM sensitivity threshold. Solid curves are for a separation of 4.33\AA between the STM tip atom and the gold film. The (black) dotted curve for $\text{C}_6\text{H}_{10}\text{S}$ is for a 5.05\AA separation.

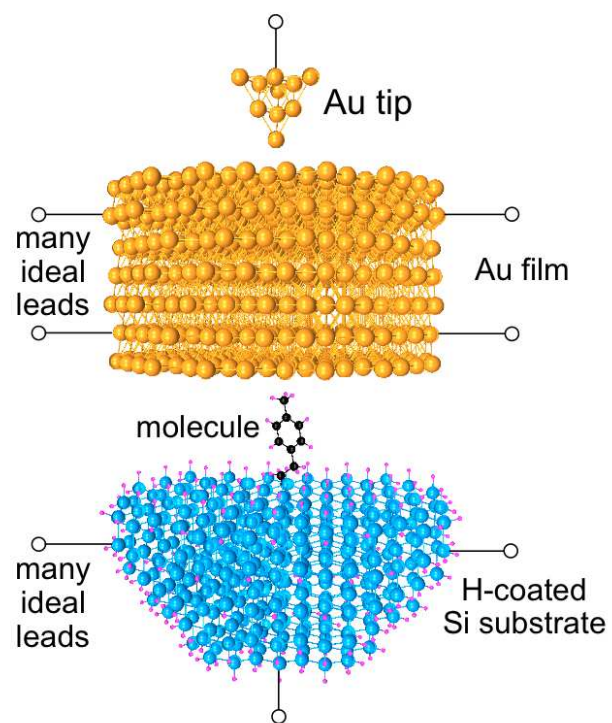


Fig.1
Kirczenow

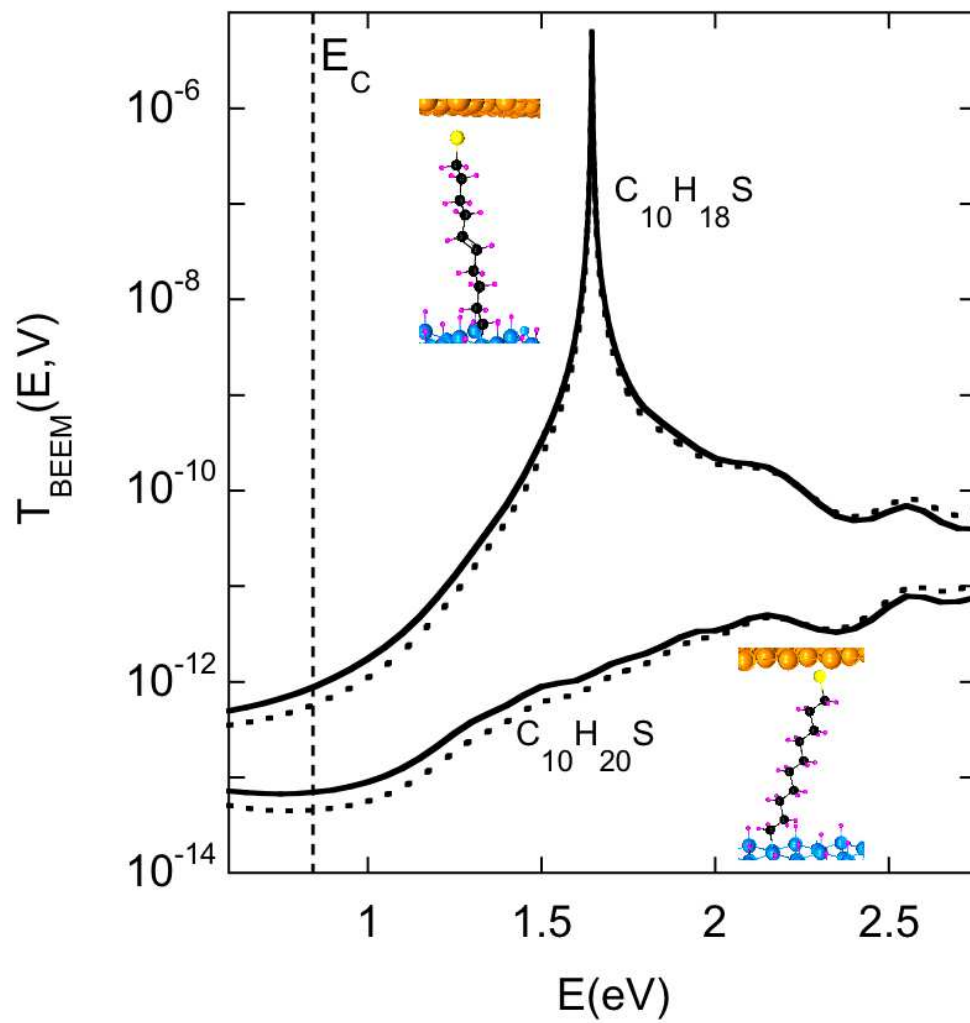


Fig.2
Kirczenow

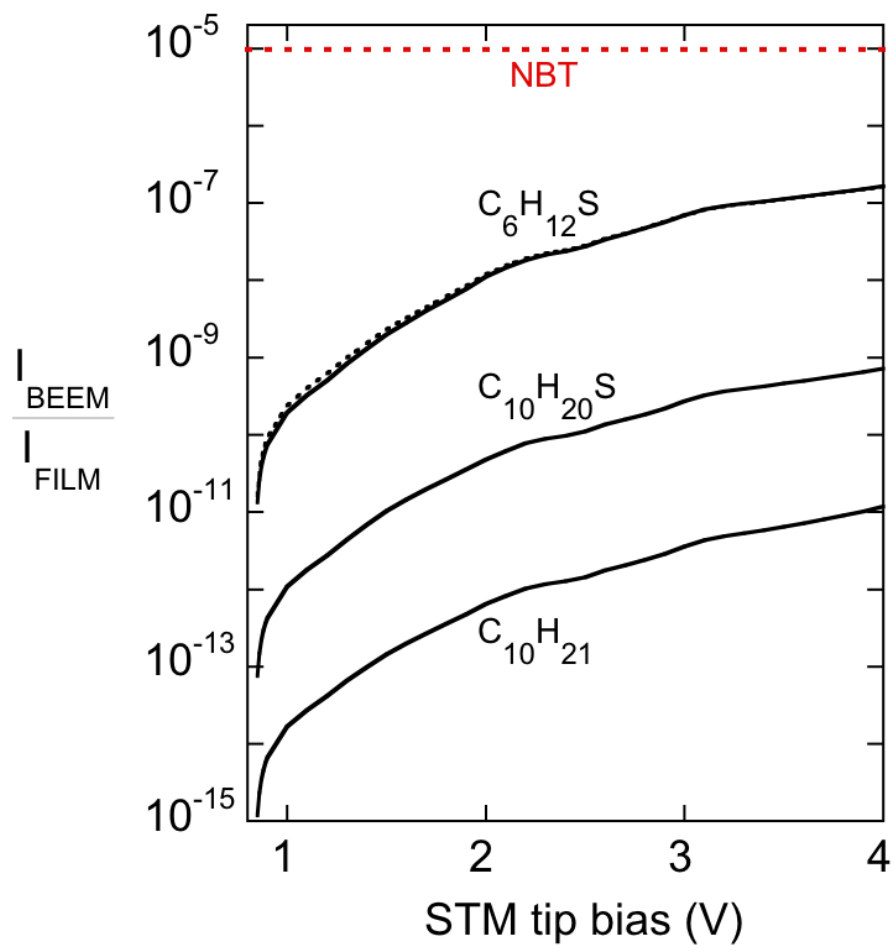


Fig. 3
Kirczenow

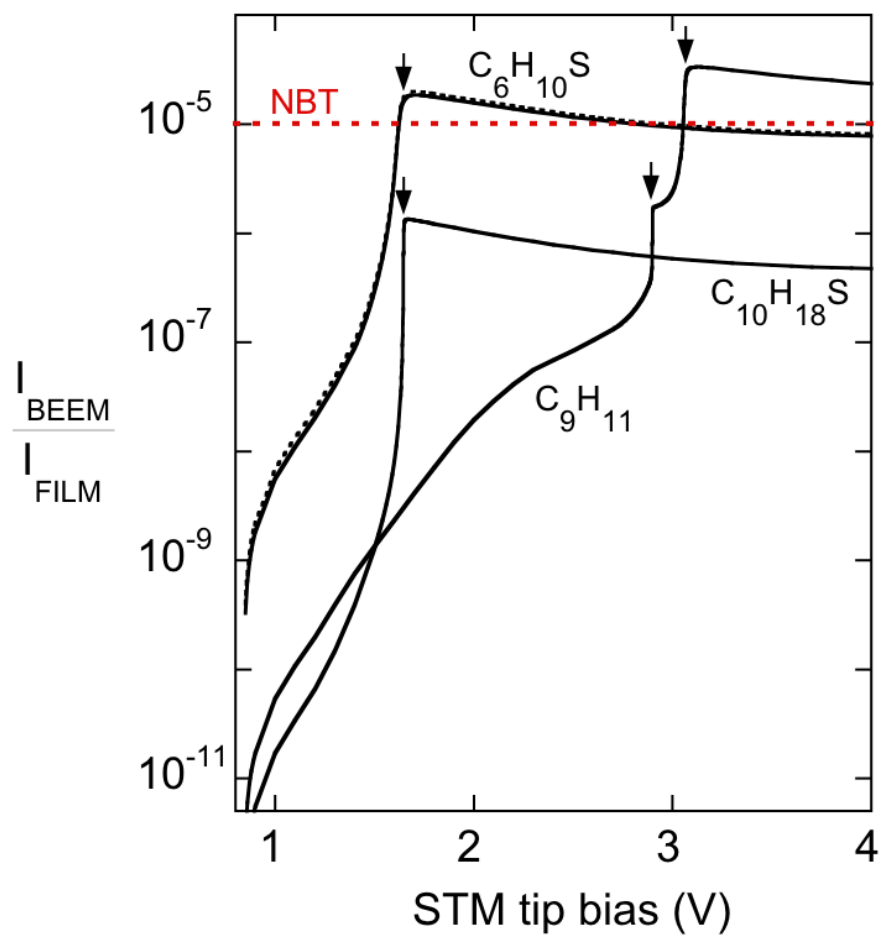


Fig. 4
Kirczenow